A SUBSPACE APPROACH TO SPECTRAL QUANTIFICATION FOR MR SPECTROSCOPIC IMAGING

BY

YUDU LI

THESIS

Submitted in partial fulfillment of the requirements
for the degree of Master of Science in Electrical and Computer Engineering
in the Graduate College of the
University of Illinois at Urbana-Champaign, 2017

Urbana, Illinois

Adviser:

Professor Zhi-Pei Liang

ABSTRACT

The problem of spectral quantification for magnetic resonance spectroscopic imaging (MRSI) is addressed in this thesis. We present a novel approach to solving this problem, incorporating both spatial and spectral prior information. More specifically, a new signal model is proposed which represents the spectral variations of each molecule as a subspace and the entire spectrum as a union-of-subspaces. The proposed model enables an efficient computational framework to quantify the unknown spectral parameters using both spectral and spatial prior information. Particularly, based on this model, the spectral quantification can be solved in two steps: (1) subspace estimation based on the empirical distributions of the spectral parameters obtained by initial spectral quantification imposing the spectral constraints, and (2) parameter estimation for the union-of-subspaces model imposing the spatial constraints. The proposed method has been evaluated using both simulated and experimental data, producing very impressive results. The resulting algorithm is expected to be useful for any metabolic imaging studies using MRSI.

In this thesis, background materials including a brief review of the existing spectral quantification methods are firstly presented. Then the proposed subspace spectral model is introduced followed by a detailed description of the resulting quantification algorithm. Finally, spectral quantification results from both simulated and *in vivo* MRSI data are presented to demonstrate the performance of the proposed method.

To my parents, for their love and support.

ACKNOWLEDGMENTS

My sincerest appreciation goes first to my advisor Dr. Zhi-Pei Liang, who supported and encouraged me throughout the course of this research and also my graduate education. His unwavering enthusiam for science and technologies kept me constantly engaged in my research and study.

My gratitude also extends to my laboratory colleagues. Dr. Fan Lam's suggestions and encouragement have been very valuable in completing this work. Thanks also go to Rong Guo and Bryan Clifford, who helped me to acquire the experimental data used in this thesis and also shared their insights about this field.

Finally, I would like to thank my family and my many close friends for their love, undestanding and support.

TABLE OF CONTENTS

CHAPTER 1

INTRODUCTION

1.1 Problem Formulation

Spectral quantification for magnetic resonance spectroscopic imaging (MRSI) is addressed in this thesis. Specifically, we assume that the measured MRSI signal at spatial location $\boldsymbol{x}$ with L molecules is represented as

$$d(\boldsymbol{x},t)=\sum_{\ell=1}^{L}c_{\ell}(\boldsymbol{x})\phi_{\ell}(\boldsymbol{\beta}(\boldsymbol{x}),t)+n(\boldsymbol{x},t), \tag{1.1}$$

where $c_{\ell}(\boldsymbol{x})$ denotes the molecular concentration for the ℓ^{th} molecule, $\phi_{\ell}(\boldsymbol{\beta},t)$ is the corresponding spectral basis function and $n(\boldsymbol{x},t)$ is the additive noise. The functional form of $\phi_{\ell}(\boldsymbol{\beta},t)$ can be obtained either from quantum mechanical simulation or experiments while $\boldsymbol{\beta}$ is to compensate the spectral variations under different experimental conditions [1]. The problem of spectral quantification is to derive the quantitative molecular information from the measured MRSI data. In practice, molecular concentrations are adequate for most applications, therefore the objective of this work is to accurately estimate the parameters $\{c_{\ell}\}_{\ell=1}^{L}$ in Eq. (1.1).

1.2 Motivation

Magnetic resonance spectroscopic imaging is a unique tool for non-invasive, label-free molecular imaging (i.e., without using exogenous contrast agents).

In contrast to magnetic resonance imaging (MRI) that collects signals from only the water molecules, MRSI acquires spatially resolved spectra, which contain information from various physiologically important molecules (e.g., metabolites and neurotransmitters) [2]. With this capability, MRSI promises to significantly impact many applications, from early detection of diseases like tumors [3–5] to basic scientific studies on metabolism [6, 7]. Most applications require quantitative derivation of molecular information, which makes spectral quantification a crucial step in MRSI. However, obtaining accurate spectral estimates is rather challenging due to the low signal-to-noise ratios (SNR) of the measured data, especially for high resolution acquisitions and the nonlinearity of the underlying optimization problem [1].

While many computational solutions have been proposed to address the problem of spectral quantification in recent decades, among the most popular are parametric approaches [8–12] incorporating spectral prior information which absorb the spectral priors in the form of spectral basis functions that can be obtained from either quantum mechanical simulations [13–15] or *in vitro* experiments. Spectral priors of this nature provide much stronger constraints compared to those used in the linear prediction based methods [16,17], improving the spectral estimation. However, these methods quantify the MRSI data for each spatial location independently and the estimation variances are often too large to be useful in practice, particularly for high resolution MRSI. To address this problem, some recent MRSI quantification methods have also incorporated the spatial prior information, which proves to significantly reduce the underlying estimation uncertainty [18–21]. Nevertheless, such formulation often leads to solving a large nonlinear optimization problem, which suffers from severe computational complexity, preventing these solutions from practical use. Given the importance of spectral quantification to quantitative metabolic imaging studies using MRSI and

the limitations of the current approaches, a new method which can effectively and efficiently incorporate both spectral and spatial prior information is demanded.

1.3 Main Results

In this work, we propose a new framework to solve the spectral quantification problem for MRSI, which effectively incorporates both spatial and spectral prior knowledge in a computationally efficient way. The main results of this work are summarized as follows.

Firstly, we propose a novel signal model for MRSI which represents the spectral distribution for each molecule as a subspace (instead of a parametric function) and the entire spectrum as a union-of-subspaces. This new representation transforms the formulation of spectral estimation from a nonlinear problem into a linear one, which enables effective and efficient incorporation of spatio-spectral priors.

Secondly, with the proposed model, we develop a computational algorithm which solves the problem in two steps: (1) subspace estimation for individual molecules based on their empirical distributions, and (2) parameter estimation by solving a linear least-squares problems with incorporation of spatial regularization.

Finally, the proposed approach has been evaluated using both simulated and experimental data, producing significantly improved estimation results. We believe the resulting algorithm will be useful for any quantitative metabolic studies using MRSI.

1.4 Organization of the Thesis

This thesis is organized as follows:

Chapter 2 is devoted to a literature review. Several existing spectral quantification methods are discussed, including the linear prediction based methods, methods imposing spectral constraints alone and methods imposing both spectral and spatial constraints. The weakness and strengths of each method are also discussed.

In Chapter 3, the proposed subspace signal model is introduced. More specifically, the motivation of the proposed model is first given, followed by the definition and characteristics of the proposed model. The model is also justified heuristically using a computational simulation. Moreover, incorporation of spatial prior information into the proposed model has also been discussed using the Bayesian estimation theory.

Chapter 4 presents the resulting spectral quantification algorithm enabled by the proposed subspace model. Particularly, the proposed method solves the spectral quantification problem in two steps: (1) subspace estimation based on the empirical distributions of the spectral parameters imposing the spectral constraints, and (2) parameter estimation imposing the spatial constraints.

In Chapter 5, the performance of the proposed method is analyzed based on spectral quantification results from both simulated and real experimental MRSI data.

Chapter 6 concludes this thesis.

CHAPTER 2

BACKGROUND

2.1 Linear Prediction Based Methods

From spin physics, the spectroscopy signal with L' spectral components (or peaks in the spectral domain) can be modeled as a linear combination of exponential functions:

$$d(t_m) = \sum_{\ell'=1}^{L'} c_{\ell'} e^{i2\pi \triangle f_{\ell'} t_m} e^{-t_m/T_{2,\ell'}} + \xi(t_m), m = 0, 1, ..., M-1, \tag{2.1}$$

where $\{c_{\ell'}\}_{\ell'=1}^{L'}$ are linear coefficients related to spin densities, $\{\triangle f_{\ell'}\}_{\ell'=1}^{L'}$ are the frequency shifts and $\{T_{2,\ell'}\}_{\ell'=1}^{L'}$ are the relaxation times and $\xi(t_m)$ is the noise (often Gaussian and white in practice). Based on Eq. (2.1), obtaining the optimal parameters in a maximum likelihood sense entails solving the following optimization problem:

$$\min_{c_{\ell'}, \triangle f_{\ell'}, T_{2,\ell'}} \sum_{m=1}^{M} ||d(t_m) - \sum_{\ell'=1}^{L'} c_{\ell'} e^{i2\pi \triangle f_{\ell'} t_m} e^{-t_m/T_{2,\ell'}}||_2^2. \tag{2.2}$$

The problem in Eq. (2.2) is often a complex nonlinear problem with many local minima where common nonlinear least-squares optimization methods often result in high computational complexity and poor performance.

However, the signal model in Eq. (2.1) adopts a similar formulation to those used in classic harmonic retrieval problems. Therefore, harmonic retrieval

algorithms based on linear predictability can be used to efficiently solve the problem in Eq. (2.2) with reasonable performance. A number of harmonic retrieval methods have been proposed, such as Prony's method [22], Tufts and Kumaresan method [16, 23, 24] and Hankel singular value decomposition (HSVD) [17]. Among these methods, the Tufts and Kumaresan method and HSVD become the most popular methods for spectral quantification in the field of magnetic resonance spectroscopy (MRS) or MRSI. In this thesis, we give a brief review of the HSVD algorithm. The Tufts and Kumaresan method shares the similar spirit of HSVD; readers may refer to [16].

The HSVD algorithm assumes the signals are uniformly sampled with sampling interval $\triangle t$ (i.e., $t_m = m\triangle t$) and estimates the unknown parameters in Eq. (2.1) from the measured data in a non-iterative fashion. For simplicity, we rewrite the measured spectroscopy signal in a more compact form:

$$d_m = \sum_{\ell'=1}^{L'} c_{\ell'} z_{\ell'}^m + \xi_m, \tag{2.3}$$

where $z_{\ell'} = e^{i2\pi\triangle f_{\ell'}\triangle t} e^{-\triangle t/T_{2,\ell'}}$, $d_m = d(m\triangle t)$ and $\xi_m = \xi(m\triangle t)$. Instead of directly solving a nonlinear least-squares problem, HSVD manipulates a 2D Hankel matrix $\mathbf{D}$ formed by the measured data as

$$\mathbf{D} = \begin{bmatrix} d_0 & d_1 & \dots & d_{M'} \\ d_1 & d_2 & \dots & d_{M'+1} \\ \vdots & \vdots & \ddots & \vdots \\ d_K & d_{K+1} & \dots & d_{M-1} \end{bmatrix}, \tag{2.4}$$

where $K = M - M' - 1$. The fact that $\{d_m\}_{m=0}^{M-1}$ have the linear predictability of order L' without the existence of noise ensures that the corresponding $\mathbf{D}$ should have a rank of L' and can be decomposed using singular value decomposition [17]:

$$\mathbf{D} = \mathbf{U}_{L'} \Lambda_{L'} \mathbf{V}_{L'}, \tag{2.5}$$

in which $\Lambda_{L'}$ is an $L' \times L'$ sigular value matrix, $\mathbf{U}_{L'}$ is the left singular vector matrix and $\mathbf{V}_{L'}$ is the right singular vector matrix. In practice, the rank of $\mathbf{D}$ is often much larger than L' in the presence of noise and Eq. (2.5) no longer holds. In this case, the decomposition in Eq. (2.5) is performed on the rank-L' approximation of $\mathbf{D}$ instead.

On the other hand, it can be ascertained that $\mathbf{D}$ can also be factorized by (in the noiseless case) [17]:

$$\mathbf{D} = \mathbf{D}_{left}\mathbf{D}_{right} = \begin{bmatrix} \tilde{\boldsymbol{e}} \\ \tilde{\boldsymbol{e}}\mathbf{Z} \\ \vdots \\ \tilde{\boldsymbol{e}}\mathbf{Z}^K \end{bmatrix} \begin{bmatrix} \boldsymbol{c} & \mathbf{Z}\boldsymbol{c} & \dots & \mathbf{Z}^{M'}\boldsymbol{c} \end{bmatrix}, \tag{2.6}$$

where $\tilde{\boldsymbol{e}}$ is a row vector whose elements are all ones, $\mathbf{Z}$ is an $L' \times L'$ diagonal matrix whose diagonal entries are $\{z_{\ell'}\}$ and $\boldsymbol{c}$ is a column vector composed of $\{c_{\ell'}\}$. Note that the factorization in Eq. (2.5) and Eq. (2.6) are related through a non-singular matrix $\mathbf{Q}$, which leads to the estimation of $\mathbf{Z}$ by diagonalizing $\mathbf{U}_b^+ \mathbf{U}_t$, where $\mathbf{U}_b$ and $\mathbf{U}_t$ denote the matrices with the bottom and top rows removed from $\mathbf{U}_{L'}$ respectively, and $(\cdot)^+$ denotes the Moore-Penrose psudo-inverse. With $\mathbf{Z}$ determined, $\{z_{\ell'}\}$ can be extracted from its diagonal, which in turn yields the estimation of $\{\triangle f_{\ell'}\}$ and $\{T_{2,\ell'}\}$.

Although HSVD solves the nonlinear optimization problem in a computationally efficient way and usually performs well when the measured data have high SNR, its estimation accuracy will largely reduce when the noise increases significantly, which is often the case in practice, especially for MRSI studies. This is because the underlying degrees of freedom is often very large

for Eq. (2.1), which results in large estimation uncertainty when the SNR is low. In addition, HSVD is a biased estimator in the presence of noise since the low-rank truncation would introduce undesired bias into the estimates.

2.2 Spectral Quantification Imposing Spectral Constraints

A major limitation of the spectral quantification methods based on Eq. (2.1) is its large degrees of freedom (i.e., L' is usually a large number in practice), which leads to large estimation variances especially when the SNR is low. To address this issue, incorporation of the spectral prior information is often necessary. A popular approach to achieving this is to impose the spectral constraints in the form of predetermined spectral basis functions [8–12]. More specifically, the single voxel spectroscopy signal with L molecules are modeled as

$$d(t_m) = \sum_{\ell=1}^{L} c_\ell e^{i2\pi \triangle f_\ell t_m} e^{-t_m/T_{2,\ell}} \tilde{\phi}_\ell(t_m) + \xi(t_m), m = 0, 1, ..., M-1, \quad (2.7)$$

where $\tilde{\phi}_\ell(\cdot)$ is the spectral basis function for the ℓ^{th} molecule, $\triangle f_\ell$ is the corresponding frequency shift and $T_{2,\ell}$ is the relaxation time. This model can be derived from Eq. (2.1) with the assumption that the spectral components associated with the same molecule have the same relaxation parameter. To see this, we explicitly express $\{\tilde{\phi}_\ell(\cdot)\}_{\ell=1}^{L}$ as

$$\tilde{\phi}_\ell(t_m) = \sum_{\ell''=1}^{L''} c_{\ell''} e^{i2\pi \triangle f_{\ell''} t_m}, \quad (2.8)$$

where L'' denotes the number of specrtal components associated with the ℓ^{th} metabolite. As can be seen, absorbing Eq. (2.8) into Eq. (2.1) leads

to the signal model in Eq. (2.7) with $\{\triangle f_\ell\}_{\ell=1}^{L}$ accounting for the overall frequency shifts. However, instead of estimating $\{c_{\ell''}\}_{\ell''=1}^{L''}$ and $\{\triangle f_{\ell''}\}_{\ell''=1}^{L''}$ from the noisy data as in the linear prediction based method, these unknown parameters can be predetermined by either *in vitro* experiments or quantum mechanical simulations [13–15]. Figure 2.1 illustrates two examples of the spectral basis functions obtained from simulations shown in [25]. With the spectral basis functions predetermined, the underlying degrees of freedom have been largely reduced in that L is usually very small compared to L', which leads to significantly improved estimation accuracy as reported in [9–12].

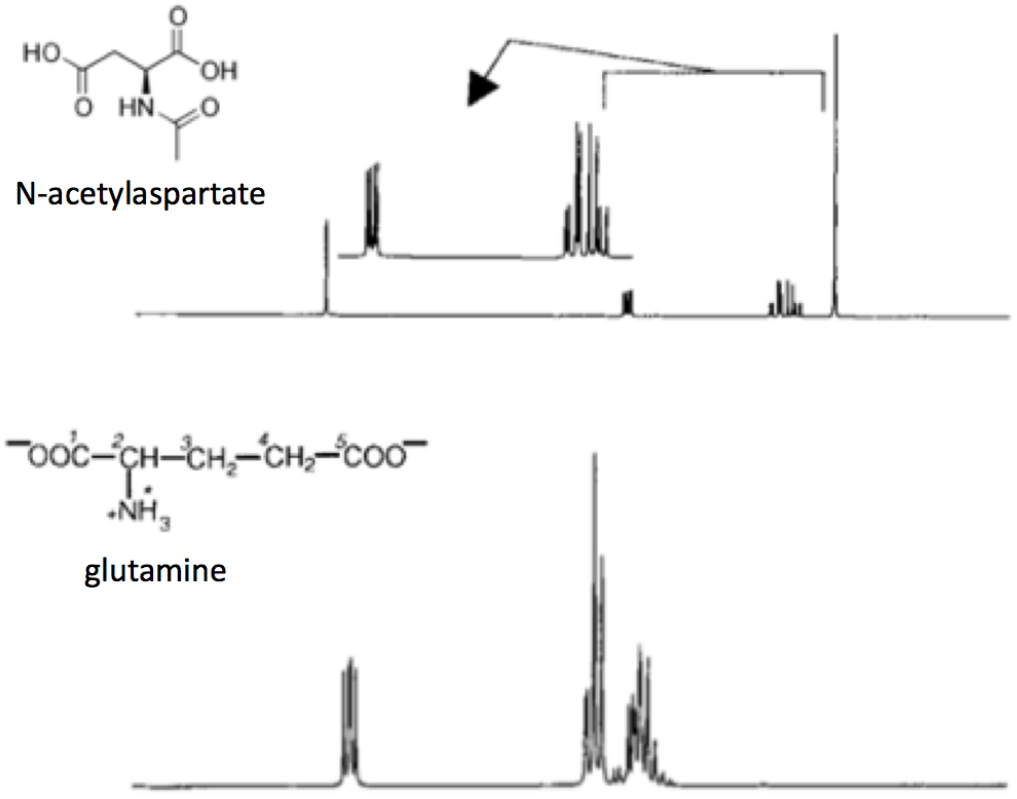

Figure 2.1: Spectral basis functions for N-acetylaspartate and glutamine, respectively, as is shown in [25].

The formulation in Eq. (2.7) results in a maximum likelihood estimation

by solving

$$\min_{c_\ell, \triangle f_\ell, T_{2,\ell}} \sum_{m=1}^{M} ||d(t_m) - \sum_{\ell=1}^{L} c_\ell e^{i2\pi \triangle f_\ell t_m} e^{-t_m/T_{2,\ell}} \tilde{\phi}_\ell(t_m)||_2^2. \tag{2.9}$$

An efficient way to solve this optimization problem is to apply the variable projection strategy [26, 27] where the estimation of the nonlinear parameters is decoupled from that of the linear parameters, significantly reducing the computational complexity.

2.3 Spectral Quantification Imposing Spatial Constraints

In spectral quantification for MRSI, exploitation of spectral prior information alone (i.e., solving the optimization problem in Eq. (2.11) voxel-by-voxel) is often inadequate, as the SNR is usually even lower especially for high resolution acquisitions. Much effort has been made to further improve the quantification accuracy for MRSI, by exploiting prior information along spatial directions. To this end, the state-of-the-art methods all share the same strategy where the use of spatial regularization is adopted to implicitly impose the spatial constraints [18–21]. More specifically, they solve the following regularized least-squares problem jointly for all the voxels:

$$\begin{aligned} \min_{c_\ell, \triangle f_\ell, T_{2,\ell}} \sum_{m=1}^{M} ||d(\boldsymbol{x}, t_m) - \sum_{\ell=1}^{L} c_\ell(\boldsymbol{x}) e^{i2\pi \triangle f_\ell(\boldsymbol{x}) t_m} e^{-t_m/T_{2,\ell}(\boldsymbol{x})} \tilde{\phi}_\ell(t_m)||_2^2 \\ +\lambda R(\{c_\ell\}, \{\triangle f_\ell\}, \{T_{2,\ell}\}), \end{aligned} \tag{2.10}$$

where $R(\cdot)$ is some regularization function and λ is the tunable parameter. An alternative view of spatial regularization is based on the well-known Bayesian estimation theory where the prior distributions of the unknown pa-

rameters are known [28]. In the sense of maximum a posteriori (MAP), the optimal estimates should maximize the following quantity:

$$ln(P(\boldsymbol{d}|\{c_\ell\},\{\triangle f_\ell\},\{T_{2,\ell}\})) + ln(P(\{c_\ell\},\{\triangle f_\ell\},\{T_{2,\ell}\})), \tag{2.11}$$

where $\boldsymbol{d}$ is composed of the measured data. In the case of Gaussian white noise, this formulation is equivalent to Eq. (2.10).

Many spatial regularization functions have been explored, such as the one that corresponds to the Gaussian Markov random field prior [20], weighted-L_2 function [29] and total variation function [21, 29]. While most spatial priors have significantly improved the spectral quantification for MRSI, the optimization in Eq. (2.10) often results in heavy computational complexity because of its high-dimensionality of the searching space and nonlinearity.

CHAPTER 3

THEORY

3.1 Subspace Spectral Model

The conventional spectral model represents the noiseless spectroscopic signal with L compounds (or molecules) as

$$s(t) = \sum_{\ell=1}^{L} c_\ell \phi_\ell(\boldsymbol{\beta}, t), \tag{3.1}$$

where c_ℓ denotes the molecular concentration for the ℓ^{th} component and $\phi_\ell(\boldsymbol{\beta}, t)$ is the corresponding spectral basis function [1]. In the context of MRSI, both c_ℓ and $\phi_\ell(\boldsymbol{\beta}, t)$ depend on the spatial location, therefore the spectroscopic imaging signal can be expressed as

$$s(\boldsymbol{x}, t) = \sum_{\ell=1}^{L} c_\ell(\boldsymbol{x}) \phi_\ell(\boldsymbol{\beta}(\boldsymbol{x}), t). \tag{3.2}$$

The functional form of the spectral basis function can be obtained from either quantum simulations or *in vitro* experiments where the parameters $\boldsymbol{\beta}$ are used to accommodate the spectral variations under practical conditions (e.g., lineshape and frequency shifts, etc.). With this signal representation, the spectral quantification is often formulated as a challenging nonlinear problem. Conventional methods determine $c_\ell(\boldsymbol{x})$ and $\boldsymbol{\beta}(\boldsymbol{x})$ for each spatial location independently and their estimation uncertainly is usually too large, especially for high resolution acquisitions with low SNR. Joint estimation of

$c_\ell(\boldsymbol{x})$ and $\boldsymbol{\beta}(\boldsymbol{x})$ for all the voxels with incorporation of spatial constraints proves to reduce the estimation variances, but it usually results in solving a highly complex nonlinear optimization problem (see Chapter 2 for details).

In this thesis, we propose a novel subspace model to represent the parametric spectral basis function for each molecule. More specifically, we assume that $\phi_\ell(\boldsymbol{\beta}, t)$ resides in a Q_ℓ-dimensional subspace spanned by $\{b_{\ell,q}(t)\}_{q=1}^{Q_\ell}$ and express $\phi_\ell(\boldsymbol{\beta}, t)$ as

$$\phi_\ell(\boldsymbol{\beta}, t) = \sum_{q=1}^{Q_\ell} a_{\ell,q} b_{\ell,q}(t). \tag{3.3}$$

The subspace model in Eq. (3.3) is motivated by the fact that the spectral distributions of an individual molecule, which are currently represented by a family of functions $\phi_\ell(\boldsymbol{\beta}, t)$, often reside in a low-dimensional subspace when the random vector $\boldsymbol{\beta}$ varies over a small range, as is often the case in practice. To heuristically justify this property, we take N-acetylaspartate (NAA), myo-inositol (mI) and glutamate (Glu) as examples. For each molecule, we generated a set of spectral functions $\{\phi(\boldsymbol{\beta_m}, t)\}_{m=1}^{M}$ (with $M = 5000$) using quantum mechanical simulations [13–15] with parameter vector $\boldsymbol{\beta}$ consisting of frequency shifts $\triangle f$ and relaxation times T_2. We further assume $\boldsymbol{\beta}$ is uniformly distributed with $\triangle f$ varies over $[-5, 5]$ Hz and T_2 varies over $[150, 350]$ ms, $[100, 300]$ ms and $[75, 275]$ ms for NAA, mI and Glu respectively according to the literature values [30]. The generated spectral functions $\{\phi(\boldsymbol{\beta_m}, t)\}_{m=1}^{M}$ are indeed highly linearly dependent for a particular molecule. To see this, we form the following Casorati matrix for each molecule using $\{\phi(\boldsymbol{\beta_m}, t)\}_{m=1}^{M}$ and calculate its corresponding singular values:

$$\mathbf{C} = \begin{bmatrix} \phi(\boldsymbol{\beta}_1, t_1) & \phi(\boldsymbol{\beta}_1, t_2) & \dots & \phi(\boldsymbol{\beta}_1, t_n) \\ \phi(\boldsymbol{\beta}_2, t_1) & \phi(\boldsymbol{\beta}_2, t_2) & \dots & \phi(\boldsymbol{\beta}_2, t_n) \\ \vdots & \vdots & \ddots & \vdots \\ \phi(\boldsymbol{\beta}_M, t_1) & \phi(\boldsymbol{\beta}_M, t_2) & \dots & \phi(\boldsymbol{\beta}_M, t_n) \end{bmatrix}. \tag{3.4}$$

Figure 3.1 illustrates the singular value distributions of the Casorati matrices. As it can be seen, the singular values correspond to each molecules decays rapidly (rank < 16 in contrast to $M = 5000$), indicating that $\{\phi(\boldsymbol{\beta}_{\boldsymbol{m}}, t)\}_{m=1}^{M}$ indeed reside in a low-dimensional subspace.

Combining the subspace representation for each spectral component, the entire spectrum can be expressed using a union-of-subspaces model:

$$s(\boldsymbol{x}, t) = \sum_{\ell=1}^{L} \sum_{q=1}^{Q_\ell} a_{\ell,q}(\boldsymbol{x}) b_{\ell,q}(t), \tag{3.5}$$

where $a_{\ell,q}$ absorbs the c_ℓ in Eq. (3.2). This union-of-subspaces representation transforms the formulation of spectral quantification from a nonlinear problem into a bilinear one. This novel representation enables effective and efficient incorporation of spatio-spectral constraints, as shown in Chapter 4.

3.2 Exploitation of Spatial Priors

Incorporation of spatial priors has been demonstrated to be useful to improve spectral quantification [18–21]. A common practice is to follow a Bayesian approach by maximizing the posterior distribution of the observed data with specific priors over the parameter maps. Under the conventional signal representation, this Bayesian formulation leads to rather complex optimization problems with spatial regularizations over the nonlinear parameters. In contrast, the proposed union-of-subspaces model enables more efficient incorpo-

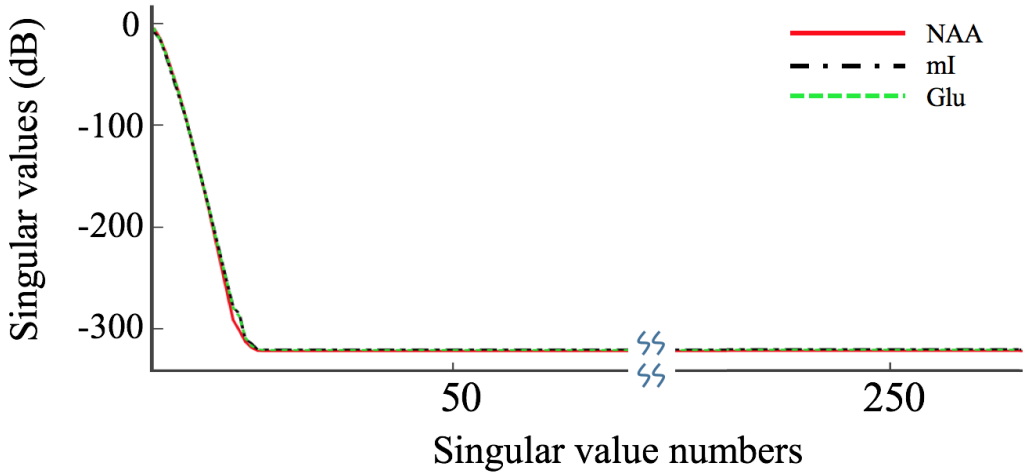

Figure 3.1: Singular value distributions of the Casorati matrices defined in Eq. (3.4) for the spectral basis functions of NAA, mI and Glu respectively. Note that the singular values decay rapidly, signifying the low-rank nature of $\mathbf{C}$. Equivalently, $\{\phi(\boldsymbol{\beta}_m, t)\}_{m=1}^{M}$ reside in a low-dimensional subspace.

ration of the spatial prior information by maximizing the following posteriors:

$$\ln(P(\boldsymbol{d}|\{a_{l,q}\})) + \ln(P(\{a_{l,q}\})), \tag{3.6}$$

where $\boldsymbol{d}$ is composed of the measured data and $\{a_{\ell,q}\}$ are the linear coefficients in Eq. (3.5). Note that the spectral estimation problem associated with formulation (3.6) only regularizes over the linear parameters, which leads to a much simpler optimization problem.

CHAPTER 4

ALGORITHM

4.1 Subspace Estimation

Estimation of the underlying subspace for each individual spectral component (or molecule) is an important step in the proposed method. This procedure requires the prior distribution $P(\boldsymbol{\beta})$ which is usually not accessible in practice. In the proposed method, we use the empirical distribution to approximate $P(\boldsymbol{\beta})$. To see this, let $\boldsymbol{\beta}_i$ denote the parameter vector associated with the spectroscopic signal at location x_i. From a particular MRSI dataset, we can have a set of such parameters obtained from every voxel, denoted as $\{\boldsymbol{\beta}_i\}_{i=1}^{I}$ (where I is the total number of voxles) which is a series of samples drawn based on $P(\boldsymbol{\beta})$. These samples determine an empirical distribution of $\boldsymbol{\beta}$ as

$$\tilde{P}(\boldsymbol{\beta} = \boldsymbol{\theta}) = \frac{1}{I} \sum_{i=1}^{I} \delta_{\{\boldsymbol{\beta}:\boldsymbol{\beta}=\boldsymbol{\theta}\}}(\boldsymbol{\beta}_i), \tag{4.1}$$

where δ_A is the indicator function of set A. The Glivenko-Cantelli theorem in statistics states that the empirical distribution in Eq. (4.1) is asymptotically identical to $P(\boldsymbol{\beta})$, which ensures $\tilde{P}(\boldsymbol{\beta})$ to be a reasonable approximation of $P(\boldsymbol{\beta})$ when I is a large number [31], as is often the case for MRSI. Therefore, the subspace for the ℓ^{th} spectral component can be estimated by the singular value decomposition of the following Casorati matrix:

$$\mathbf{C} = \begin{bmatrix} \phi(\boldsymbol{\beta}_1, t_1) & \phi(\boldsymbol{\beta}_1, t_2) & \dots & \phi(\boldsymbol{\beta}_1, t_n) \\ \phi(\boldsymbol{\beta}_2, t_1) & \phi(\boldsymbol{\beta}_2, t_2) & \dots & \phi(\boldsymbol{\beta}_2, t_n) \\ \vdots & \vdots & \ddots & \vdots \\ \phi(\boldsymbol{\beta}_I, t_1) & \phi(\boldsymbol{\beta}_M, t_2) & \dots & \phi(\boldsymbol{\beta}_I, t_n) \end{bmatrix}. \tag{4.2}$$

We choose the conjugate of the most dominant Q_ℓ right singular vectors of $\mathbf{C}$ as $\{b_{\ell,q}(t)\}_{q=1}^{Q_\ell}$. As reported in [1], Q_ℓ is selected such that the $Q_{\ell+1}$th singular value decays below -50 dB.

It remains to obtain the sample spectral functions $\{\phi_\ell(\boldsymbol{\beta}_i, t)\}_{i=1}^{I}$ for each molecule. To address this, the proposed method solves the following nonlinear optimization problem voxel-by-voxel for all the locations ($i = 1, 2, \cdots, I$):

$$\{c_{i,\ell}^*\}, \boldsymbol{\beta}_i^* = \arg \min_{\{c_{i,\ell}\}, \boldsymbol{\beta}_i} \sum_{n=1}^{N} \left\| d(\boldsymbol{x}_i, t_n) - \sum_{\ell=1}^{L} c_{i,\ell} \phi_\ell(\boldsymbol{\beta}_i, t_n) \right\|_2^2, \tag{4.3}$$

where $\{t_n\}$ are sampling indexes and $d(\boldsymbol{x}_i, t_n)$ denotes the measured noisy data correspond to $s(\boldsymbol{x}_i, t_n)$. Note that this processing step is the same as what is done in conventional parametric quantification methods (e.g., QUEST [12]) but the estimated $\{c_{i,\ell}^*\}$ and $\boldsymbol{\beta}_i^*$ are used to determine the subspace structure instead of being treated as the final estimates, as is the case in conventional methods.

It is worthwhile to note that for a fixed distribution $P(\boldsymbol{\beta})$, different trials will generate different sample values according to $P(\boldsymbol{\beta})$ such that the corresponding Casorati matrices vary as well. However, it can be proved that when the number of samples is large enough, these Casorati matrices all share the same subspace. The detailed discussion of the proof is beyond the scope of this thesis and will be addressed in future research. In addition, when the SNR of the measured data is too low as is often the case, especially for high resolution MRSI, the $\{\boldsymbol{\beta}_i^*\}_{i=1}^{I}$ as estimated in Eq. (4.3) usually results in a

biased approximation of $P(\boldsymbol{\beta})$. This problem can be handled by determining $\{\boldsymbol{\beta}_i^*\}_{i=1}^I$ at a lower spatial resolution where the SNR is improved. This strategy is reasonable since $\{\boldsymbol{\beta}_i^*\}_{i=1}^I$ are only used for subspace estimation rather than as a final estimates, which is another strength of the proposed method [1].

4.2 Spectral Quantification

Once the subspace structure (i.e., basis functions $\{b_{\ell,q}(t)\}_{q=1}^{Q_\ell}$) for each spectral compound has been determined, the problem of spectral quantification is reduced to estimation of $a_{\ell,q}$ in Eq. (3.3) from the measured data. As discussed in Chapter 3, joint estimation for all the spatial locations together with incorporation of spatial priors is desirable and proves to significantly reduce the estimation uncertainty. Some recent spectral quantification methods absorb the spatial constraints but at the cost of largely increased computational complexity. In contrast, the union-of-subspaces signal model (3.3) is a linear representation which simplifies the incorporation of spatial constraints. To see this, within the Bayesian framework (as discussed in Chapter 2), the underlying parameter estimation problem can be formulated as

$$\{a_{\ell,q}\}^* = \arg\min_{\{a_{\ell,q}\}} \ln(P(\boldsymbol{d}|\{a_{l,q}\})) + \ln(P(\{a_{l,q}\})). \tag{4.4}$$

In practice, the noise in the measured data can be assumed as being Gaussian and white, therefore the likelihood term in Eq. (4.4) can be rewritten as

$$\ln(P(\boldsymbol{d}|\{a_{l,q}\})) = \sum_{i,n} \left\| d(\boldsymbol{x}_i, t_n) - \sum_{\ell,q} a_{\ell,q}(\boldsymbol{x}_i) b_{\ell,q}(t_n) \right\|_2^2 + const. \tag{4.5}$$

To simplify the notation, we denote the linear coefficients for a particular basis as $\boldsymbol{a}_{\ell,q} = [a_{\ell,q}(\boldsymbol{x}_1), a_{\ell,q}(\boldsymbol{x}_2), ..., a_{\ell,q}(\boldsymbol{x}_I)]^T$ and the collection of all the coefficients as $\boldsymbol{a} = [\boldsymbol{a}_{1,1}^T, \boldsymbol{a}_{1,2}^T, ..., \boldsymbol{a}_{1,Q_1}^T, ..., \boldsymbol{a}_{L,1}^T, \boldsymbol{a}_{L,2}^T, ..., \boldsymbol{a}_{L,Q_L}^T]^T$ [1]. Furthermore, we represent $\ln(P(\{a_{l,q}\}))$ as a function of $\boldsymbol{a}$ and denote it as $R(\boldsymbol{a})$. With the above notation, Eq. (4.4) can be reformulated as

$$\boldsymbol{a}^* = \arg\min_{\boldsymbol{a}} \sum_{i,n} \left\| d(\boldsymbol{x}_i, t_n) - \sum_{\ell,q} a_{\ell,q}(\boldsymbol{x}_i) b_{\ell,q}(t_n) \right\|_2^2 + R(\boldsymbol{a}), \tag{4.6}$$

which is essentially a linear least-squares optimization problem with spatial regularization. While spatial priors of any form can be easily imposed into the formulation, two types of spatial constraints are the most popular: (a) weighted-L_2 regularization, and (b) total variation regularization [1]. The idea behind both formulations is to impose edge-preserving spatial smoothness onto the linear coefficients, which is motivated by the fact that in most biological samples, only limited types of tissues exist where the molecular concentrations are expected to be smooth. For weighted-L_2 regularization, $R(\boldsymbol{a})$ is chosen to be

$$R(\boldsymbol{a}) = \sum_{\ell=1}^{L} \lambda_\ell \sum_{q=1}^{Q_\ell} \|\mathbf{W}\boldsymbol{a}_{\ell,q}\|_2^2 , \tag{4.7}$$

where the λ_ℓ controls the trade-off between data-consistency and spatial smoothness while $\mathbf{W}$ is a edge-preserving weighting matrix derived from the auxilliary anatomical images [32]. For total variation regularization, $R(\boldsymbol{a})$ can be expressed by

$$R(\boldsymbol{a}) = \sum_{\ell=1}^{L} \lambda_\ell \sum_{q=1}^{Q_\ell} \|\nabla\boldsymbol{a}_{\ell,q}\|_1 , \tag{4.8}$$

where ∇ denotes the gradient operator.

In this thesis, we focus on the weighted-L_2 regularization to demonstrate the feasibility of the proposed method. Changing into total variation regularization is also within the reach since the formulation only regularizes over the linear coefficients. With weighted-L_2 regularization, the optimization problem in Eq. (4.6) becomes a quadratic programming problem and can be solved by many algorithms such as the preconditioned conjugate gradient [33].

The final concentration for the ℓ^{th} molecule (c_ℓ) can be computed as

$$c_\ell(\boldsymbol{x}) = \sum_{q=1}^{Q_\ell} a_{\ell,q}(\boldsymbol{x}) b_{\ell,q}(0). \tag{4.9}$$

This can be justified by assuming that the ℓ^{th} spectral component can be represented as

$$s_\ell(\boldsymbol{x}, t) = \sum_{q=1}^{Q_\ell} a_{\ell,q}(\boldsymbol{x}) b_{\ell,q}(t) = c_\ell(\boldsymbol{x}) e^{i2\pi \triangle f_\ell t} e^{-\alpha_\ell t} \tilde{\phi}_\ell(t), \tag{4.10}$$

where $\triangle f_\ell$ represents the frequency shift, α_ℓ is the damping factor and $\tilde{\phi}_\ell(t)$ is the basis function obtained by quantum simulation. Then c_ℓ is equivalent to $\sum_{q=1}^{Q_\ell} a_{\ell,q}(\boldsymbol{x}) b_{\ell,q}(0)$ if $\tilde{\phi}_\ell(t)$ is normalized properly.

CHAPTER 5

RESULTS AND DISCUSSION

5.1 Simulation Study

The performance of the proposed method has been evaluated and compared to two different quantification methods using 2-D MRSI simulation data. The simulated data was synthesized based on Eq. (2.7) using the spectral structures obtained from NMR-SCOPE [15], a standard software generating spectral basis functions based on quantum mechanics. The data were composed of six common molecules, namely, N-acetylaspartate (NAA), creatine (Cr), choline (Cho), myo-inositol (mI) and glutamate (Glu). The spatial distributions of the molecular concentrations and relaxation times were chosen to be smooth within each tissue (e.g., gray matter, white matter and cerebrospinal fluid) but varies across different tissue types. Considering that the inter-voxel field inhomogeneity can be effectively removed using the method proposed in [34,35] and the residual intra-voxel field inhomogeneity is usually negligible, in this study, the frequency shifts $\{\triangle f_\ell\}$ were not included. Additive Gaussian and white noise was also added into the data. The sampling bandwidth was set as 2000 Hz and the matrix size was 128×128.

The proposed method was first evaluated by a Monte-Carlo study with 40 realizations, comparing the quantification results obtained from the proposed method and QUEST which is a conventional quantification algorithm imposing only the spectral constraints [12]. Figure 5.1 illustrates the quan-

tification accuracy along spatial directions including standard deviation of the estimates from the Monte-Carlo studies and the concentration maps of different molecules estimated in one of the realizations. Figure 5.2 illustrates the quantification accuracy along the spectral direction using a set of representative spectral fitting results including the spectra synthesized from the estimated parameters and the error spectra compared to the ground truth. The figures show that the proposed method has significantly improved the estimation accuracy and reduced the spatial variations compared to QUEST, which indicates effective incorporation of both spectral and spatial prior information.

The proposed method was also compared to one of the state-of-the-art quantification methods imposing both spatial and spectral constraints proposed in [21], using a similar Monte-Carlo study. Figure 5.3 shows the estimation standard deviations in the Monte-Carlo study and the estimated concentration maps in one realization. As can be seen, the two methods achieved comparable performances both qualitatively and quantitatively in terms of relative errors for the estimated concentration maps. However, it took the method in [21] approximately 6.8 hours to produce these results while the proposed method only took about 10 minutes. As expected, the proposed method is significantly more computationally efficient.

5.2 *In Vivo* Study

To further validate the proposed method under practical conditions, two *in vivo* experiments were also conducted. The first experiment acquired a set of data from a healthy subject on a 3T Siemens Trio scanner using an echo-planar spectroscopic imaging (EPSI) sequence with water suppression [36] and outer-volume saturation [37]. The echo time was 30 ms, the echo spacing

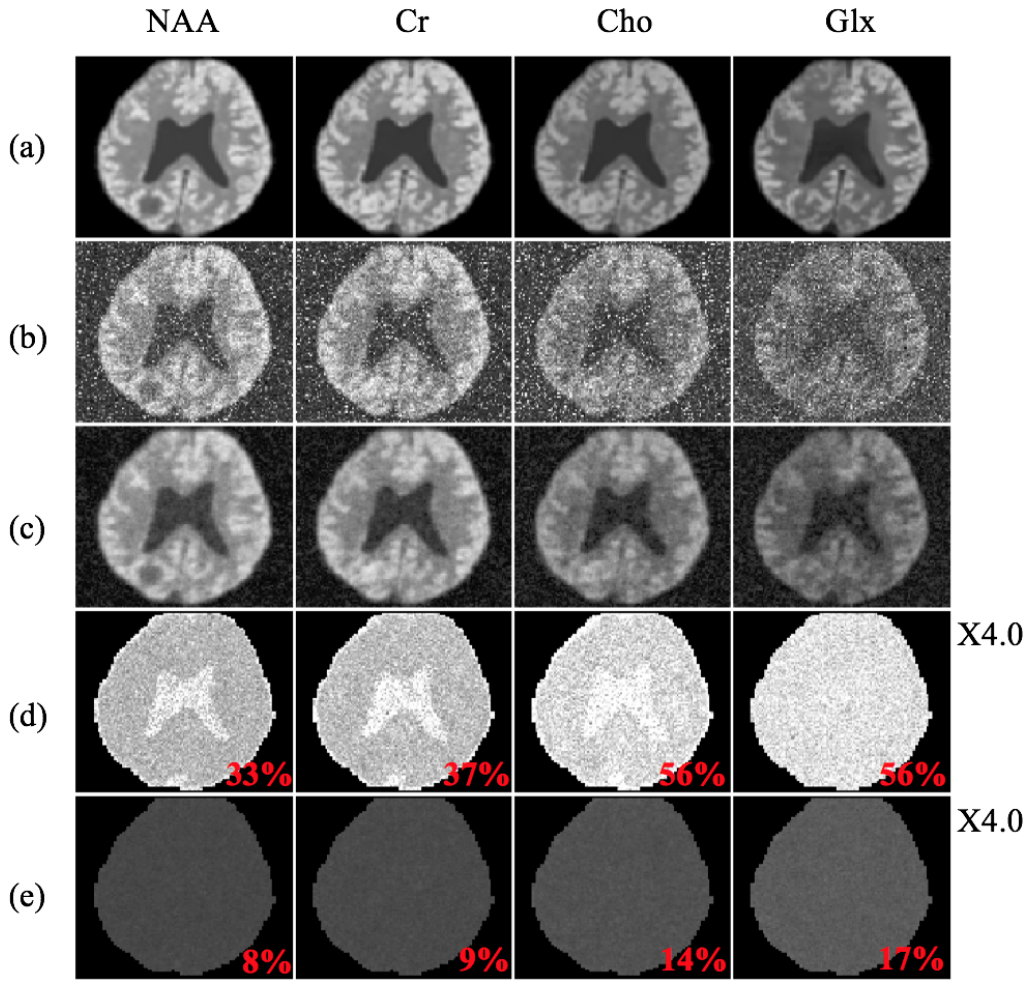

Figure 5.1: Simulation results showing the quality of spatial estimation, including (a) ground truth concentration distributions for NAA, Cr, Cho and Glx, concentration distributions estimated in one of the realizations of the Monte-Carlo study using (b) QUEST and (c) the proposed method, and standard deviation (SD) maps (normalized by the true concentrations) for (d) QUEST and (e) the proposed method. The mean SDs for individual molecules are also shown in red texts. Note the proposed method significantly improves the accuracy of the estimated concentrations compared to QUEST.

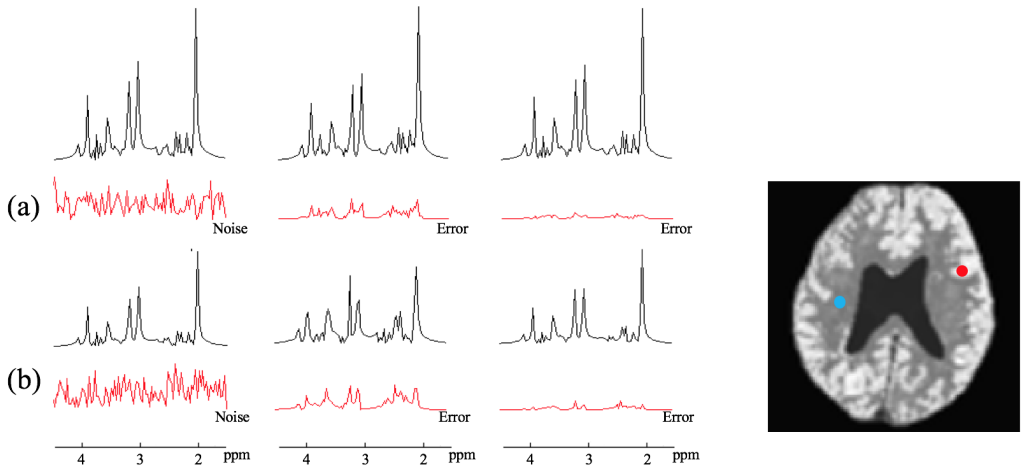

Figure 5.2: Simulation results showing the quality of spectral estimation, including spectra from two representative voxels marked by the red and blue dots shown in rows (a) and (b), respectively. The additive noise and estimation errors are also shown in red. Note the proposed method produces significantly better spectral variations than QUEST.

was 1.42 ms and the in-plane resolution was 4.6×4.6 mm^2 [1]. The residual water and lipid signals were removed using the method proposed in [38]. The inter-voxel field inhomogeneity was also corrected before quantification using the B_0 maps obtained from an auxiliary scan. Figure 5.4 compares the concentration maps estimated by QUEST and the proposed method. The figure shows that the estimates produced by QUEST have large spatial variations, which has been significantly reduced by the proposed method. These estimation results are consistent to the simulation study shown in Fig. 5.1 and Fig. 5.2.

The second experiment was designed to validate the proposed method for processing high resolution MRSI data. To this end, another set of data was acquired from a healthy subject using the recently developed SPICE

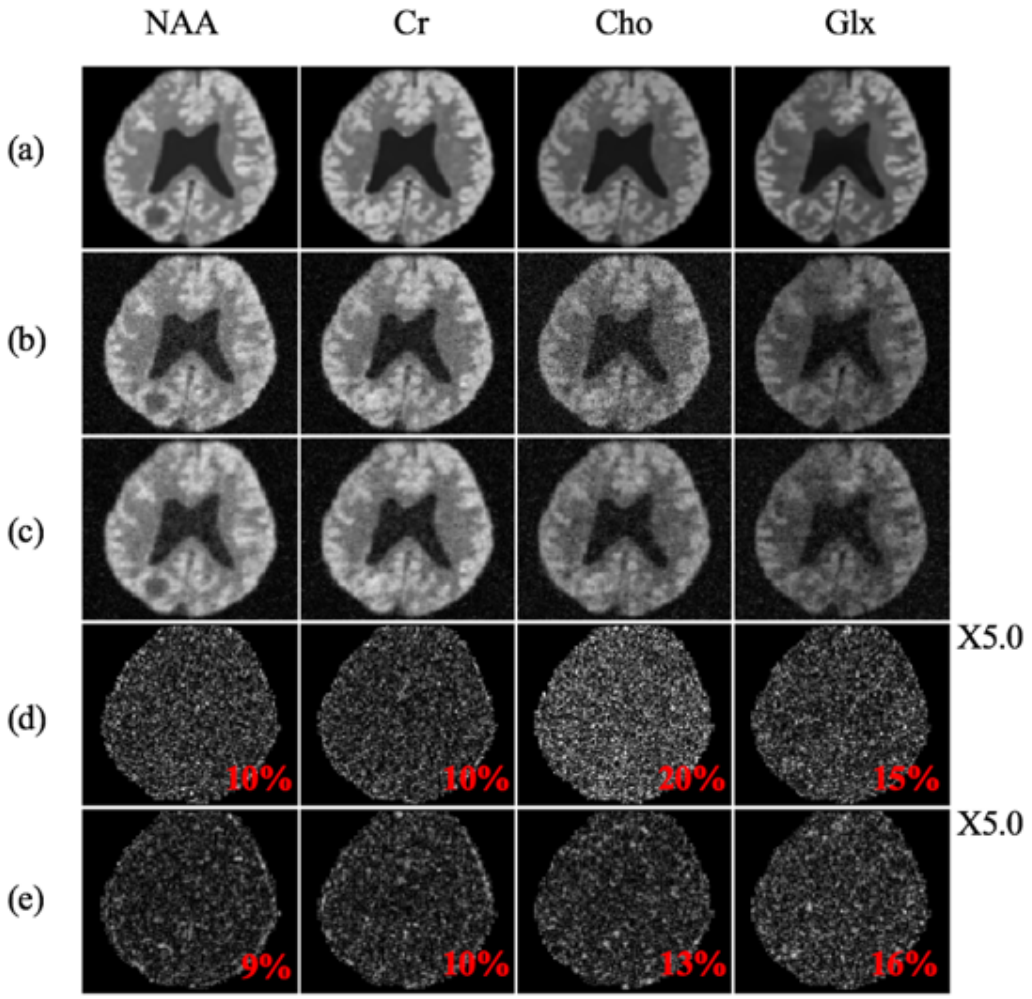

Figure 5.3: Simulation results comparing the estimated concentration maps from our previous method and the proposed method: (a) true concentration maps for NAA, Cr, Cho and Glx; (b) concentration maps estimated using the state-of-the-art method described in [21]; (c) concentration maps estimated using the proposed method; and (d-e) relative error maps for the results in (b) and (c), respectively. The average relative L2 errors for the entire brain are also shown (in red texts). Note that the computation time is around 7 hours for the previous method, and only 10 minutes for the proposed method.

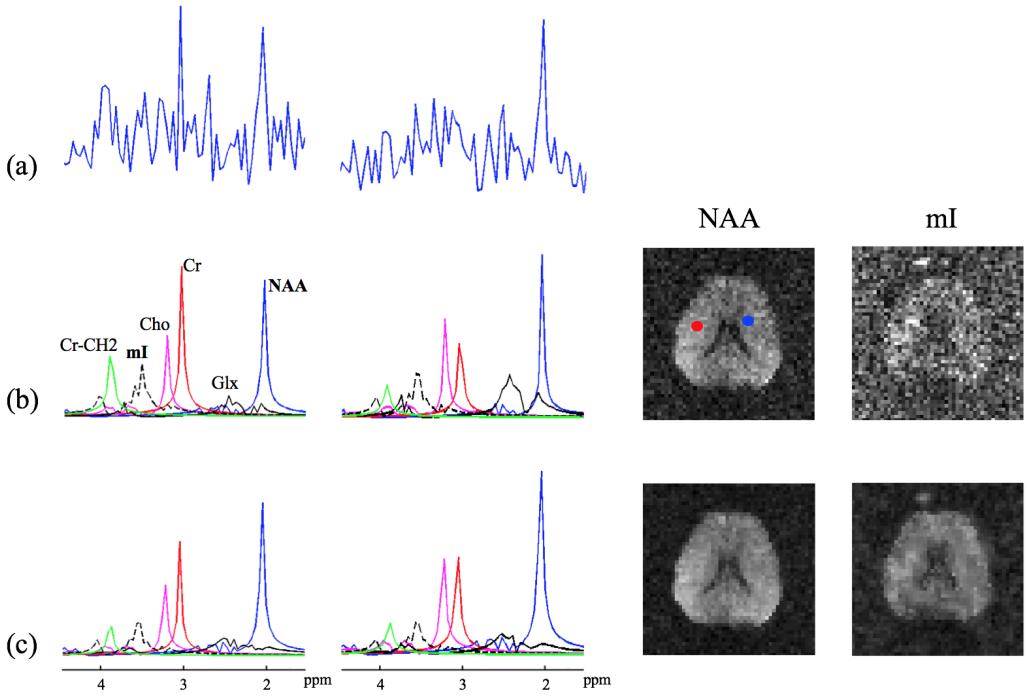

Figure 5.4: *In vivo* results from an MRSI data acquired using the EPSI sequence, including (a) noisy spectra from the voxels marked by the blue and red dots, (b) quantification results from QUEST including the synthesized individual spectral components and the concentration maps (note the mI maps are scaled by a factor of 3 for better visualization), and (c) quantification results from the proposed method.

technique [34, 39] with the following imaging parameters: 230×230 mm^2 field-of-view (FOV), 2.5×2.5 mm^2 in-plane resolution, TR/TE = 260/4 ms and 1.78 ms echo spacing. Figure 5.5 shows the quantification results from the proposed method. As it can be seen, both the concentration distributions and spectral decompositions are of high quality, which is very encouraging considered such a small voxel size.

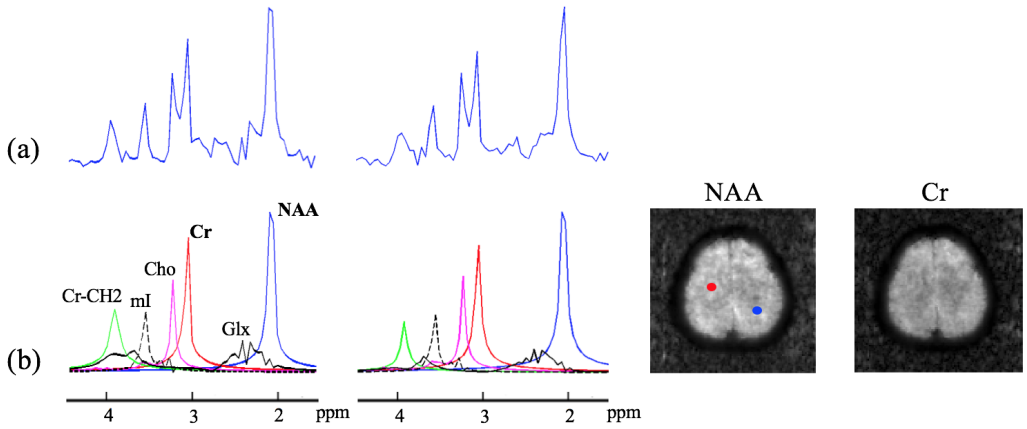

Figure 5.5: *In vivo* results from a high resolution MRSI data acquired using the SPICE technique, including (a) two spectra from the voxels marked by the blue and red dots and (b) quantification results from the proposed method including spectral decomposition and the concentration maps.

CHAPTER 6

CONCLUSIONS

The problem of spectral quantification for noisy MRSI data has been addressed in this thesis. The low SNR of the measured data and high degrees of freedom makes this problem rather challenging. Previous studies have proven that incorporation of both spatial and spectral prior information is very useful to improve the quantification accuracy. However, the current spectral models imposing spatio-spectral constraints often lead to highly complex nonlinear optimization problems which are very difficult to solve in practice. To address this issue, we present a new approach to spectral quantification for MRSI using a subspace spectral model. This novel model represents the spectral variations of each molecule using a subspace and the entire spectrum as a union-of-subspaces. The proposed model transforms the formulation of spectral quantification from a nonlinear problem into a linear one, which enables effective and efficient incorporation of prior information. The proposed method has been evaluated using both simulated and experimental data, producing very accurate quantification results in a computationally efficient way. The resulting algorithm is expected to be useful for any quantitative metabolic imaging studies using MRSI.

REFERENCES

[1] Y. Li, L. Fan, B. Clifford, and Z.-P. Liang, "A subspace approach to spectral quantification for MR spectroscopic imaging," *IEEE Transactions on Biomedical Engineering*, vol. 64, no. 10, pp. 2486–2489, 2017.

[2] R. A. De Graaf, *In vivo NMR Spectroscopy: Principles and Techniques*. John Wiley & Sons, 2013.

[3] S. J. Nelson, D. B. Vigneron, and W. P. Dillon, "Serial evaluation of patients with brain tumors using volume MRI and 3D 1H-MRSI," *NMR in Biomedicine*, vol. 12, no. 3, pp. 123–138, 1999.

[4] A. Stadlbauer, E. Moser, S. Gruber, R. Buslei, C. Nimsky, R. Fahlbusch, and O. Ganslandt, "Improved delineation of brain tumors: An automated method for segmentation based on pathologic changes of 1H-MRSI metabolites in gliomas," *Neuroimage*, vol. 23, no. 2, pp. 454–461, 2004.

[5] A. Pirzkall, X. Li, J. Oh, S. Chang, M. S. Berger, D. A. Larson, L. J. Verhey, W. P. Dillon, and S. J. Nelson, "3D MRSI for resected high-grade gliomas before RT: Tumor extent according to metabolic activity in relation to MRI," *International Journal of Radiation Oncology Biology Physics*, vol. 59, no. 1, pp. 126–137, 2004.

[6] K. Glunde, L. Jiang, S. A. Moestue, and I. S. Gribbestad, "MRS and MRSI guidance in molecular medicine: Targeting and monitoring of choline and glucose metabolism in cancer," *NMR in Biomedicine*, vol. 24, no. 6, pp. 673–690, 2011.

[7] J. O'Neill, J. Levitt, R. Caplan, R. Asarnow, J. T. McCracken, A. W. Toga, and J. R. Alger, "1H-MRSI evidence of metabolic abnormalities in childhood-onset schizophrenia," *Neuroimage*, vol. 21, no. 4, pp. 1781–1789, 2004.

[8] J. Van der Veen, R. De Beer, P. Luyten, and D. Van Ormondt, "Accurate quantification of in vivo 31P NMR signals using the variable projection method and prior knowledge," *Magnetic Resonance in Medicine*, vol. 6, no. 1, pp. 92–98, 1988.

[9] L. Vanhamme, A. van den Boogaart, and S. Van Huffel, "Improved method for accurate and efficient quantification of MRS data with use of prior knowledge," *Journal of Magnetic Resonance*, vol. 129, no. 1, pp. 35–43, 1997.

[10] J.-B. Poullet, D. M. Sima, A. W. Simonetti, B. De Neuter, L. Vanhamme, P. Lemmerling, and S. Van Huffel, "An automated quantitation of short echo time MRS spectra in an open source software environment: AQSES," *NMR in Biomedicine*, vol. 20, no. 5, pp. 493–504, 2007.

[11] L. Vanhamme, A. van den Boogaart, and S. Van Huffel, "Improved method for accurate and efficient quantification of MRS data with use of prior knowledge," *Journal of Magnetic Resonance*, vol. 129, no. 1, pp. 35–43, 1997.

[12] H. Ratiney, M. Sdika, Y. Coenradie, S. Cavassila, D. v. Ormondt, and D. Graveron-Demilly, "Time-domain semi-parametric estimation based on a metabolite basis set," *NMR in Biomedicine*, vol. 18, no. 1, pp. 1–13, 2005.

[13] S. Smith, T. Levante, B. H. Meier, and R. R. Ernst, "Computer simulations in magnetic resonance. An object-oriented programming approach," *Journal of Magnetic Resonance, Series A*, vol. 106, no. 1, pp. 75–105, 1994.

[14] B. J. Soher, K. Young, A. Bernstein, Z. Aygula, and A. A. Maudsley, "GAVA: Spectral simulation for in vivo MRS applications," *Journal of Magnetic Resonance*, vol. 185, no. 2, pp. 291–299, 2007.

[15] D. Stefan, F. Di Cesare, A. Andrasescu, E. Popa, A. Lazariev, E. Vescovo, O. Strbak, S. Williams, Z. Starcuk, M. Cabanas et al., "Quantitation of magnetic resonance spectroscopy signals: The jMRUI software package," *Measurement Science and Technology*, vol. 20, no. 10, p. 104035, 2009.

[16] H. Barkhuijsen, R. De Beer, W. Bovee, J. Creyghton, and D. Van Ormondt, "Application of linear prediction and singular value decomposition (LPSVD) to determine NMR frequencies and intensities from the FID," *Magnetic Resonance in Medicine*, vol. 2, no. 1, pp. 86–89, 1985.

[17] H. Barkhuijsen, R. De Beer, and D. Van Ormondt, "Improved algorithm for noniterative time-domain model fitting to exponentially damped magnetic resonance signals," *Journal of Magnetic Resonance (1969)*, vol. 73, no. 3, pp. 553–557, 1987.

[18] C. Sava, R. Anca, D. M. Sima, J.-B. Poullet, A. J. Wright, A. Heerschap, and S. Van Huffel, "Exploiting spatial information to estimate metabolite levels in two-dimensional MRSI of heterogeneous brain lesions," *NMR in Biomedicine*, vol. 24, no. 7, pp. 824–835, 2011.

[19] A. Laruelo, L. Chaari, J.-Y. Tourneret, H. Batatia, S. Ken, B. Rowland, R. Ferrand, and A. Laprie, "Spatio-spectral regularization to improve magnetic resonance spectroscopic imaging quantification," *NMR in Biomedicine*, vol. 29, no. 7, pp. 918–931, 2016.

[20] B. M. Kelm, F. O. Kaster, A. Henning, M.-A. Weber, P. Bachert, P. Boesiger, F. A. Hamprecht, and B. H. Menze, "Using spatial prior knowledge in the spectral fitting of MRS images," *NMR in Biomedicine*, vol. 25, no. 1, pp. 1–13, 2012.

[21] Q. Ning, C. Ma, F. Lam, and Z.-P. Liang, "Spectral quantification for high-resolution MR spectroscopic imaging with spatiospectral constraints," *IEEE Transactions on Biomedical Engineering*, vol. 64, no. 5, pp. 1178–1186, 2017.

[22] S. Kunis, T. Peter, T. Römer, and U. von der Ohe, "A multivariate generalization of Prony's method," *Linear Algebra and Its Applications*, vol. 490, pp. 31–47, 2016.

[23] D. Tufts and R. Kumaresan, "Singular value decomposition and improved frequency estimation using linear prediction," *IEEE Transactions on Acoustics, Speech, and Signal Processing*, vol. 30, no. 4, pp. 671–675, 1982.

[24] R. Kumaresan and D. W. Tufts, "Estimating the angles of arrival of multiple plane waves," *IEEE Transactions on Aerospace and Electronic Systems*, no. 1, pp. 134–139, 1983.

[25] V. Govindaraju, K. Young, and A. A. Maudsley, "Proton NMR chemical shifts and coupling constants for brain metabolites," *NMR in Biomedicine*, vol. 13, no. 3, pp. 129–153, 2000.

[26] G. H. Golub and V. Pereyra, "The differentiation of pseudo-inverses and nonlinear least squares problems whose variables separate," *SIAM Journal on Numerical Analysis*, vol. 10, no. 2, pp. 413–432, 1973.

[27] G. H. Golub and V. Pereyra, "Separable nonlinear least squares: The variable projection method and its applications," *Inverse Problems*, vol. 19, no. 2, p. R1, 2003.

[28] H. L. Van Trees, *Detection, Estimation, and Modulation Theory.* John Wiley & Sons, 2004.

[29] Q. Ning, C. Ma, and Z.-P. Liang, "Spectral estimation for magnetic resonance spectroscopic imaging with spatial sparsity constraints," in *Biomedical Imaging (ISBI), 2015 IEEE 12th International Symposium on*. IEEE, 2015, pp. 1482–1485.

[30] F. Träber, W. Block, R. Lamerichs, J. Gieseke, and H. H. Schild, "1H metabolite relaxation times at 3.0 tesla: Measurements of T1 and T2 values in normal brain and determination of regional differences in transverse relaxation," *Journal of Magnetic Resonance Imaging*, vol. 19, no. 5, pp. 537–545, 2004.

[31] H. G. Tucker, "A generalization of the Glivenko-Cantelli theorem," *The Annals of Mathematical Statistics*, vol. 30, no. 3, pp. 828–830, 1959.

[32] J. P. Haldar, D. Hernando, S.-K. Song, and Z.-P. Liang, "Anatomically constrained reconstruction from noisy data," *Magnetic Resonance in Medicine*, vol. 59, no. 4, pp. 810–818, 2008.

[33] S. C. Eisenstat, "Efficient implementation of a class of preconditioned conjugate gradient methods," *SIAM Journal on Scientific and Statistical Computing*, vol. 2, no. 1, pp. 1–4, 1981.

[34] F. Lam and Z.-P. Liang, "A subspace approach to high-resolution spectroscopic imaging," *Magnetic Resonance in Medicine*, vol. 71, no. 4, pp. 1349–1357, 2014.

[35] Y. Liu, C. Ma, B. A. Clifford, F. Lam, C. L. Johnson, and Z.-P. Liang, "Improved low-rank filtering of magnetic resonance spectroscopic imaging data corrupted by noise and B_0 field inhomogeneity," *IEEE Transactions on Biomedical Engineering*, vol. 63, no. 4, pp. 841–849, 2016.

[36] A. Haase, J. Frahm, W. Hanicke, and D. Matthaei, "1H NMR chemical shift selective (CHESS) imaging," *Physics in Medicine and Biology*, vol. 30, no. 4, p. 341, 1985.

[37] P. Le Roux, R. J. Gilles, G. C. McKinnon, and P. G. Carlier, "Optimized outer volume suppression for single-shot fast spin-echo cardiac imaging," *Journal of Magnetic Resonance Imaging*, vol. 8, no. 5, pp. 1022–1032, 1998.

[38] C. Ma, F. Lam, C. L. Johnson, and Z.-P. Liang, "Removal of nuisance signals from limited and sparse 1H MRSI data using a union-of-subspaces model," *Magnetic Resonance in Medicine*, vol. 75, no. 2, pp. 488–497, 2016.

[39] F. Lam, C. Ma, B. Clifford, C. L. Johnson, and Z.-P. Liang, "High-resolution 1H-MRSI of the brain using SPICE: Data acquisition and image reconstruction," *Magnetic Resonance in Medicine*, vol. 76, no. 4, pp. 1059–1070, 2016.